This article has been accepted for publication in a future issue of this journal, but has not been fully edited. Content may change prior to final publication. Citation information: DOI 10.1109/TII.2018.2818153, IEEE Transactions on Industrial Informatics

Generalized Proportional Integral Observer-Based Robust Finite Control Set Predictive Current Control for Induction Motor Systems with Time-Varying Disturbances

Junxiao Wang, *Member, IEEE,* Fengxiang Wang[1], *Member, IEEE,* Gaolin Wang, *Member, IEEE,* Shihua Li, *Senior Member, IEEE,* Li Yu, *Member, IEEE,*

***Abstract*—During the past few years, finite control set predictive current control (PCC) method has attracted more and more attention in research and industry applications. However, PCC method could be improved by considering two points. Firstly, the current reference used in the cost function of PCC control scheme is usually produced by a proportional and integration (PI) speed controller. Confront with load torque and time varying system parameters, it is a better solution to design a disturbance estimation based feed-forward compensated controller. In this way, the current reference could be generated faster and more accurate. Secondly, the PCC method is model based method which means the accuracy of the model parameters are essential. In real system, time varying parameters existed almost always. This paper investigates a generalized proportional integral observer (GPIO)based PCC approach for dealing with load torque disturbance, time-varying parameter uncertainties. The effectiveness of the proposed method has also been confirmed by simulation and a lab-constructed experimental prototype.**

***Index Terms*—Generalized proportional integral observer (GPIO), finite control set predictive current control (PCC), disturbance rejection, induction motor.**

This work was supported in part by National Natural Science Foundation (NNSF) of China under Grants (61473080, 51507172, U1709213) and Fujian Engineering and Research Center of Electrical Drives and Power Electronics. (1. Corresponding author: Fengxiang Wang.)

Junxiao Wang is with the College of Information Engineering, Zhejiang University of Technology, Hangzhou, 310023, China, and also with the Key Laboratory of Measurement and Control of Complex Systems of Engineering, Ministry of Education, School of Automation, Southeast University, Nanjing, China, 210096(e-mail:wangjunxiao19860128@126.com).

Fengxiang Wang is with Quanzhou Institute of Equipment Manufacturing, Haixi Institute, Chinese Academy of Sciences, Jinjiang, 362200, China(email:fengxiang.wang@fjirsm.ac.cn).

Gaolin Wang is with the Department of Electrical Engineering, Harbin Institute of Technology, Harbin, China(email:wanggaolin08@163.com).

Shihua Li is with the Key Laboratory of Measurement and Control of Complex Systems of Engineering, Ministry of Education, School of Automation, Southeast University, Nanjing, Jiangsu 210096, China(email:lsh@seu.edu.cn).

Li Yu is with the College of Information Engineering, Zhejiang University of Technology, Hangzhou, 310023, China(email:lyu@zjut.edu.cn).

I. Introduction

The control of alternating current (AC) machines is one of the most classical and challenging problems for electrical engineering [1]-[3]. In the present scenario with high development of renewable wind energy and electric cars, this problem is still of highest interest for the industrial and academic communities [5]-[6], [11], [21].

In the present control communities, considering the finite switch state character of voltage inverter, finite control set direct model predictive control (FCS-MPC) is proposed, it is also an alternating one for drive systems [15]. Different from continuous model predictive control, FCS-MPC method does not need modulator. The switching signals are generated directly via the calculation a cost function. FCS-MPC has many advantages like intuitive concept, fast dynamics, nonlinear and multi-variable solutions, system constraints included and so on. FCS-MPC has already been widely investigated and researched in power electronics [4]-[11]. For AC drives, both finite control set predictive torque control (PTC) and PCC methods do not use the cascaded PI controllers [11]. The inner current PI controller is removed, which increase the possibility of faster dynamics. However, the outer speed PI controller uses the integral method to solve the unknown load torque and parameter uncertainties, which is a slow solution. Furthermore, PTC and PCC are model based strategies [12]-[13]. The load disturbance and uncertainties of the model result in predictive methods prone to instabilities in real systems, which remains remains an important concern [14]-[15].

In recent years, due to the undesirable influences of external perturbation and system parameter uncertainties, many researchers have taken more interest in disturbance estimation based feedforward compensation methods [17]-[23], [27]. Extended state observer (ESO) is the main part of active disturbance reject control (ADRC) scheme, it regards the lumped disturbances as an extended system state and observes both system states and disturbances . The estimated value is employed for feed-forward compensation, so it could improve the system's anti-disturbance performance [20]-[21]. The generalized proportional integral

This article has been accepted for publication in a future issue of this journal, but has not been fully edited. Content may change prior to final publication. Citation information: DOI 10.1109/TII.2018.2818153, IEEE Transactions on Industrial Informatics

observer (GPIO) can provide an excellent disturbance estimation and does not require exact knowledge of the system. Unlike ESO which is only applicable for constant or slowly varying disturbance estimation, the GPIO observer can estimate many kinds of disturbances only if they can be described in time-dependant terms [24]. In addition, disturbance observer based control (DOBC) has also been proved to be effective in attenuating the effects of unknown perturbations, it has been applied in two-link robotic manipulator systems [23], PMSM servo systems [22], and so on. The major advantage of DOBC method is that the closed-loop system's disturbance rejection ability is improved without sacrificing its nominal control performance.

In this paper, aiming to improve the system performance with load torque disturbances and time-varying parameter uncertainties, the proposed disturbance estimation based feed-forward compensation is a promising solution[19]-[26]. A GPIO observer-based PCC method is developed to completely counteract the time-varying load torque disturbances and uncertainties found in induction motor systems. The contribution of our research could be summarized as:

- In the cost function of PCC control system, the current reference plays a key role for improving the system performance. Based on the disturbance compensation technique, the current reference can be generated faster and more precisely when the load torque is injected suddenly and the inertial value is time varying. With this method, the speed and torque have better behaviors refers to the system uncertainties.
- Additionally, the model parameter uncertainties also influence the accuracy of stator current and flux estimation. Unlike integral control which is only for constant disturbances, for induction machine system, the parameter uncertainties are not constant for induction machine systems, they varies with the operation temperature etc. GPIO observer could estimate the time varying parameters and unknown disturbances.
- Both in simulation and test results, the proposed method is validated to have very good convergence performance and a wide robustness range with the load disturbance and parameter variations.

This paper is organized as follows. Section II briefly revisits the induction motor system and two level voltage inverter model. The GPIO observers and compensated PCC controller are designed in Section III. In Section IV, the effectiveness of the proposed controller is obtained by numerical simulation and a lab-scaled experimental prototype. Conclusions are drawn in the end.

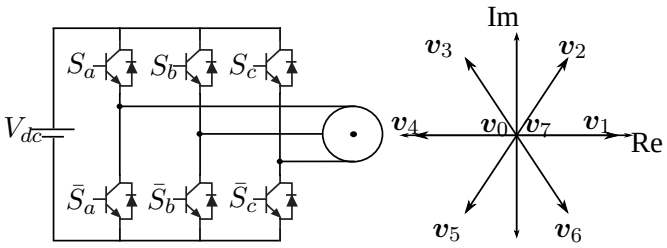

Fig. 1: inverter topology and voltage vectors.

II. MODEL DESCRIPTION OF INDUCTION MOTOR AND INVERTER

A squirrel-cage induction motor (IM) could be described by a set of nonlinear equations using a stator reference frame as follows [11],

$$\upsilon_s = R_s \cdot i_s + \frac{d}{dt}\psi_s \tag{1}$$

$$0 = R_r \cdot i_r + \frac{d}{dt}\psi_r - j \cdot \omega_e \cdot \psi_r \tag{2}$$

$$\psi_r = L_r \cdot i_r + L_m \cdot i_s \tag{3}$$

$$\psi_s = L_s \cdot i_s + L_m \cdot i_r \tag{4}$$

$$\frac{d\omega}{dt} = \frac{3pL_m\psi_r}{2L_rJ} i_q - \frac{T_L}{J} - \frac{B\omega}{J} \tag{5}$$

$$T_e = \frac{3}{2} \cdot p \cdot Im(\psi_s^* \cdot i_s) \tag{6}$$

where ψ_s and ψ_r are the stator flux and rotor flux, respectively; υ_s is the stator voltage vector. i_s and i_r are the stator and rotor currents, respectively. L_s, L_r and L_m are stator, rotor and mutual inductances, respectively; ω, and ω_e are the mechanical and electrical speeds, respectively. R_s and R_r are the stator and rotor resistances, respectively. p is the number of pole pairs, and T_L represents the load torque.

A two-level voltage source inverter and its voltage vectors are shown as Fig.1. The vector can be used to express the switching state S as follows:

$$S = \frac{2}{3}(S_a + aS_b + a^2S_c) \tag{7}$$

where $a = e^{j2\pi/3}$, $S_i = 1$ means S_i is on and $\bar{S}_i = 0$ means $\bar{S}_i$ is off, and $i = a, b, c$, $\bar{S}_i$ denotes the state of switch under the bridge arm as Fig.1. The voltage υ_s is related to the switching state S by

$$\upsilon_s = V_{dc}S \tag{8}$$

where V_{dc} is the DC link voltage.

Considering the natural switched character of inverter, it has 8 possible switching vectors and can produce only 7 output voltage vectors, the so-called finite control set model predictive control (FCS-MPC) is proposed.

This article has been accepted for publication in a future issue of this journal, but has not been fully edited. Content may change prior to final publication. Citation information: DOI 10.1109/TII.2018.2818153, IEEE Transactions on Industrial Informatics

III. GPIO BASED PREDICTIVE CURRENT CONTROLLER DESIGN

The GPIO observer-based predictive current control scheme (GPIO-PCC) for the induction motor system is presented in this section. The control structure is described in Fig. 2. The induction motor is denoted as IM, three phases currents and speed information are injected into the proposed controller. Using GPIO observers, the flux and current in rotating frame could be estimated. The predictive control consists of two parts. One is the variable prediction, the other is design of cost function which is for the selection of the optimized vectors.

A. GPIO Observer Design

A GPIO estimator is designed for observing the lumped disturbances caused by unknown load torque and mismatched parameter variations in this section. Based on the speed mathematical model (5), the equation can be rewritten as $\dot{\omega} = k_t i_q^* + d_\omega(t), k_t = \frac{3pL_{m0}\psi_r}{2L_{r0}J_0}$, where the lumped disturbance $d_\omega(t)$ is defined as $d_\omega(t) = -\frac{3pL_{m0}\psi_r}{2L_{r0}J_0}i_q^* + \frac{3pL_m\psi_r}{2L_rJ}i_q - \frac{T_L}{J} - \frac{B\omega}{J}$. The disturbance estimation $\hat{d_\omega}(t)$ is obtained by the GPIO observer which is designed as:

$$\begin{cases} \dot{z}_1 = k_t i_q^* + z_2 + \beta_1(\omega - z_1) \\ \dot{z}_2 = z_3 + \beta_2(\omega - z_1) \\ \quad \vdots \\ \dot{z}_m = \beta_m(\omega - z_1). \end{cases} \tag{9}$$

where $z_1 = \hat{\omega}, z_2 = \hat{d}_\omega(t), ...$ and $\beta_{1\ldots m} > 0$.

Assumption 3.1: For the system (5), suppose that lumped disturbance signal $d_\omega(t)$ is differentiable and $d_\omega^{(m)}(t)$ satisfies $\lim_{t\to 0} d_\omega^{(m)}(t) = 0$.

Lemma 3.1: [28] Suppose the nonlinear system

$$\dot{x} = F(x, w) \tag{10}$$

satisfies globally input-to-state stable (ISS). In addition, if the control input satisfies

$$\lim_{t\to 0} w(t) = 0, \tag{11}$$

then the control system states satisfy $\lim_{t\to 0} x(t) = 0$.

For stability analysis of GPIO observer (9), define

$$\begin{cases} e_1(t) = \omega - z_1 \\ \quad \vdots \quad \vdots \\ e_m(t) = d_\omega^{(m)}(t) - z_m \end{cases} \tag{12}$$

combining speed model and equation (9) and taking the time derivative of $e_1(t), \ldots, e_m(t)$, it yields

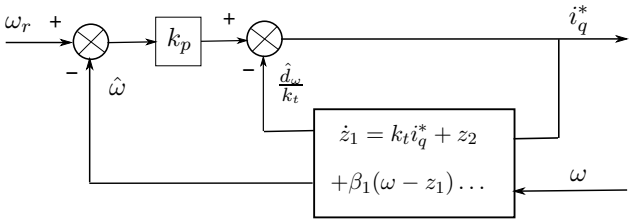

Fig. 3: Diagram of current reference i_q^* generation based on the GPIO observer.

$$\begin{cases} \dot{e}_1(t) = e_2 - \beta_1 e_1 \\ \dot{e}_2(t) = e_3 - \beta_2 e_1 \\ \quad \vdots \quad \vdots \\ \dot{e}_m(t) = d_\omega^{(m)} - \beta_m e_1. \end{cases} \tag{13}$$

The above eq. (13) could be rewritten as

$$\dot{X} = A \cdot X + D \tag{14}$$

where

$$A = \begin{bmatrix} -\beta_1 & 1 & & \ldots \\ -\beta_2 & & 1 & \ldots \\ \vdots & & & \vdots \\ -\beta_m & & \ldots & 1 \end{bmatrix} \tag{15}$$

$$D = \begin{bmatrix} \vdots \\ d_\omega^{(m)}(t) \end{bmatrix} \tag{16}$$

Since the induction motor system satisfies Assumption 3.1 and A is Hurwitz, then the error system (13) is ISS. Noting that $\lim_{t\to 0} d_\omega^{(m)}(t) = 0$, according to Lemma 3.1, we could conclude that $\lim_{t\to 0} e_1(t) = 0, \cdots, \lim_{t\to 0} e_m(t) = 0$, the error states of system (13) will converge to the desired equilibrium point asymptotically.

B. Rotor Flux and Current Observers

The proposed GPIO-PCC control scheme is described as Fig. 2, we could find that the cost function plays the key part in this predictive control algorithm. The next-step rotor flux $\hat{\psi}_r(k+1)$ and the current $\hat{i}_s(k+1)$ must be calculated for the cost function of PCC method. Considering the parameter uncertainties and time-delay of system states, the GPIO observer technique is also used for improving system robustness. The design procedure of flux and current observers is explained in detail in this section.

On the basis of the current value by measurement and voltage information, combining Eqs. (2)-(4), the rotor flux observer is designed as (17)

This article has been accepted for publication in a future issue of this journal, but has not been fully edited. Content may change prior to final publication. Citation information: DOI 10.1109/TII.2018.2818153, IEEE Transactions on Industrial Informatics

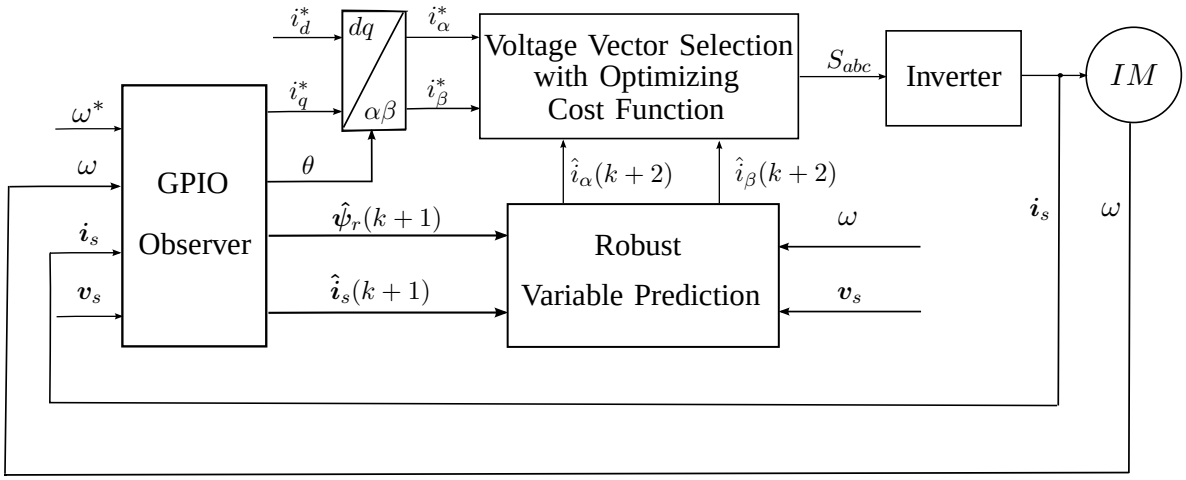

Fig. 2: Block diagram of generalized proportional integral observer based robust predictive current control scheme.

$$\begin{cases} \frac{d}{dt}\hat{\psi}_r = \frac{L_m R_r}{L_r}\cdot i_s - (\frac{R_r}{L_r} - j\cdot\omega_e)\cdot\hat{\psi}_r \\ \qquad + K_{\psi_{rp}}(\psi_r - \hat{\psi}_r) + \hat{d}_{\psi_r} \\ \dot{\hat{d}}_{\psi_r} = \hat{d}_{\psi_{r1}} + K_{\psi_{ri}}(\psi_r - \hat{\psi}_r) \\ \quad\vdots \qquad \vdots \\ \dot{\hat{d}}_{\psi_{rm}} = K_{\psi_{rim}}(\psi_r - \hat{\psi}_r) \end{cases} \tag{17}$$

Using Euler discretization, the discrete time rotor flux observer is described as

$$\begin{cases} \hat{\psi}_r(k+1) = \hat{\psi}_r(k) + T_s(-(\frac{R_r}{L_r} - j\cdot\omega_e)\cdot\hat{\psi}_r(k) + \\ \frac{L_m R_r}{L_r}T_s\cdot i_s(k) + K_{\psi_{rp}}T_s(\psi_r(k) - \hat{\psi}_r(k)) + T_s\hat{d}_{\psi_r}(k) \\ \hat{d}_{\psi_r}(k+1) = \hat{d}_{\psi_r}(k) + T_s\hat{d}_{\psi_{r1}}(k) + T_s K_{\psi_{ri}}(\psi_r(k) \\ \qquad -\hat{\psi}_r(k)) \\ \qquad\vdots \qquad \vdots \\ \hat{d}_{\psi_{rm}}(k+1) = \hat{d}_{\psi_{rm}}(k) + T_s K_{\psi_{rim}}(\psi_r(k) - \hat{\psi}_r(k)) \end{cases}$$

where T_s is the sampling period.

The stator current observer is designed as follows,

$$\begin{cases} \dot{\hat{i}}_s = -\frac{L_m^2 R_r}{(L_m^2 - L_r L_s)L_r}i_s + \frac{L_r}{L_m^2 - L_r L_s}R_s i_s \\ \qquad - \frac{L_r}{L_m^2 - L_r L_s}\upsilon_s - \frac{L_m}{L_m^2 - L_r L_s}(\frac{R_r}{L_r - j\omega})\hat{\psi}_r \\ \qquad \hat{d}_{i_s} + K_{i_{sp}}(i_s - \hat{i}_s) \\ \dot{\hat{d}}_{i_s} = \hat{d}_{i_{s1}} + K_{i_{si}}(i_s - \hat{i}_s) \\ \quad\vdots \qquad \vdots \\ \dot{\hat{d}}_{i_{sm}} = K_{i_{sim}}(i_s - \hat{i}_s) \end{cases}$$

and the discrete time stator current observer is described as

$$\begin{cases} \hat{i}_s(k+1) = (1 - \frac{T_s L_m^2 R_r}{(L_m^2 - L_r L_s)L_r})\hat{i}_s(k) + \\ \qquad \frac{T_s L_r}{L_m^2 - L_r L_s}R_s\hat{i}_s(k) - \frac{T_s L_r \upsilon_s(k)}{L_m^2 - L_r L_s} \\ \qquad - \frac{T_s L_m}{L_m^2 - L_r L_s}(\frac{R_r}{L_r - j\omega})\hat{\psi}_r(k) \\ \qquad \hat{d}_{i_s}(k) + K_{i_{sp}}(i_s(k) - \hat{i}_s(k)) \\ \hat{d}_{i_s}(k+1) = \hat{d}_{i_s}(k) + T_s\hat{d}_{i_{s1}}(k) + T_s K_{i_{si}}(i_s(k) \\ \qquad -\hat{i}_s(k)) \\ \qquad\vdots \qquad \vdots \\ \hat{d}_{i_{sm}}(k+1) = \hat{d}_{i_{sm}}(k) + T_s K_{i_{si}}(i_s(k) - \hat{i}_s(k)) \end{cases} \tag{18}$$

Define $e_{i_s} = i_s - \hat{i}_s, e_{d_{i_s}} = d_{i_s} - \hat{d}_{i_s}, e_{\psi_r} = \psi_r - \hat{\psi}_r, e_{d_{\psi_r}} = d_{\psi_r} - \hat{d}_{\psi_r}$. By combining Eqs. (17)-(18) and the system model(1)-(4), then the error system can be described as

$$\begin{cases} \dot{e}_{\psi_r} = e_{d_{\psi_r}} - (\frac{R_r}{L_r} - j\cdot\omega_e)e_{\psi_r} - K_{\psi_{rp}}e_{\psi_r} \\ \dot{e}_{d_{\psi_r}} = e_{d_{\psi_{r1}}} - K_{\psi_{ri}}e_{\psi_r} \\ \quad\vdots \qquad \vdots \\ \dot{e}_{d_{\psi_{rm}}} = d_{\psi_{rm}} - K_{\psi_{rim}}e_{\psi_r} \\ \dot{e}_{i_s} = e_{d_{i_s}} - \frac{T_s L_m}{L_m^2 - L_r L_s}(\frac{R_r}{L_r - j\omega})e_{\psi_r} - K_{i_{sp}}e_{i_s} \\ \dot{e}_{d_{i_s}} = e_{d_{i_{s1}}} - K_{i_{si}}e_{i_s} \\ \quad\vdots \qquad \vdots \\ \dot{e}_{d_{i_{sm}}} = d_{i_{sm}} - K_{i_{sim}}e_{i_s} \end{cases} \tag{19}$$

Error system (19) could also be described as $\dot{\bar{X}} = \bar{A}\bar{X} + \dot{\bar{D}}$, so its stability analysis is similar to the above section which also satisfies the ISS stability.

This article has been accepted for publication in a future issue of this journal, but has not been fully edited. Content may change prior to final publication. Citation information: DOI 10.1109/TII.2018.2818153, IEEE Transactions on Industrial Informatics

C. Predictive Current Controller Design

According to the specific control goals and system constraints, the flexible cost function could be designed. In this research, it includes three items: α and β current errors (α and β denotes stator reference frame, it could be transformed from dq frame or abc frame using the measured three phase information), and over current protection, i.e.

$$g_j = \sum_{h=1}^{N} \{|i_\alpha^* - \hat{i}_\alpha(k+h)_j| + |i_\beta^* - \hat{i}_\beta(k+h)_j| + I_m(k+h)_j\} \quad (20)$$

There are no weight factors for $\hat{i}_\alpha$ and $\hat{i}_\beta$ here, they are are equally weighted, it means that the relative importance is the same. The meaning is that we ensure that the three phase currents have the same good quality. It is also convenient for engineer to use in industry application. In addition, we do not want to add a coefficient to cost function of PCC system, which will bring the unbalance of the three phase currents, which is not expected. In the cost function g_j, $h = 2$ and j indicate the prediction horizon and the index of applied voltage vector for the prediction, respectively. There are eight different switching states for the employed two-level voltage source inverter, but it has only seven different voltage vectors to be considered. For instance in this GPIO-PCC method, $j = 0, ...6.$, that is to say, in order to select the most optimal switching state, notice that the cost function must be calculated for seven times in each predict control interval.

From (20) and (23), to complete the design of the proposed GPIO-PCC method in Fig. 2, it is necessary to transform the current references in dq frame. The block diagram of the current reference i_q^* is generated by a GPIO observer-based feed-forward compensated controller as shown in Fig. 3. The i_d^* is calculated by the rotor flux reference, it could be considered as a constant value. The corresponding reference current values i_d^* and i_q^* for generating the flux and torque, are produced by:

$$i_d^* = \frac{|\boldsymbol{\psi}_r^*|}{L_m}, \quad (21)$$

$$i_q^* = k_p(\omega_r - \hat{\omega}) - \frac{z_2}{k_t} \quad (22)$$

In the cost function, the current values in $\alpha\beta$ frame are obtained by the inverse Park transformation which is presented as follows:

$$\begin{pmatrix} \alpha \\ \beta \end{pmatrix} = \begin{pmatrix} cos(\theta) & -sin(\theta) \\ sin(\theta) & cos(\theta) \end{pmatrix} \begin{pmatrix} d \\ q \end{pmatrix} \quad (23)$$

where θ is the rotating angle.

In addition, the predicted stator current $\hat{i}_s(k+h)$ can be predicted based on the Eqs.(17)-(18). The over current protection is activated suppose the predicted current absolute value $|\hat{i}(k+h)|$ is larger than its limited value i_{max}. The current limitation is defined as

$$I_m(k+h) = \{0, if|\hat{i}(k+h)| \leq |i_{max}|, r \gg 0\} \quad (24)$$

If the condition is hold, the cost function will prevent the voltage vector from being chosen. The safety of the motor control system is guaranteed even the current is greater than i_{max}.

Remark 3.1. For the cost function of PCC method, the current reference generating accuracy and rate are very important and influence the closed-loop control performance. The existing current reference signal which is generated by a PI controller in traditional PCC scheme [11]. Because the load torque and other parameter uncertainties are unknown, the integral term can compensate the load torque and parameter uncertainties which either vary slowly or maintain constant values. However parameter uncertainties are usually time-varying, do not approach to a constant value, as is the case in resistance variation caused by operating temperature. From natural consideration which is similar to dead beat control, if the time-varying disturbances or uncertainties are measured, then the current reference can be produced as soon as possible based on disturbance feed-forward compensation. The proposed GPIO observer technique is inspired by this motivation, especially when the disturbances are time-varying, it can estimate the load torque and time-varying parameter uncertainties. The convergence rate is then ensured by tuning the observer parameters.

Remark 3.2. The parameter regulation should be compromised for the system performance. Suppose the controller parameter value k_p in speed loop is large, then it has fast response, but the undesired overshoot is brought in. The same law with observer parameters (e.g., $\beta_1, \beta_2, \cdots$) , if their value are chosen to be large, the left half plane poles are further away, then the convergence rate could be fast and disturbance reject ability is good. On the contrary, if the values are overlarge, it may lead noise into the closed-loop system, then the output fluctuation is obvious. In addition, due to the hardware limitation and computation complexity, the one-step prediction is performed in our research. As described in [15]-[16], the multi-step predictive method has been studied, it concluded that long prediction horizons could improve the system steady state performance such as reducing the switching frequency, the current total harmonic distortion (THD), and so on.

This article has been accepted for publication in a future issue of this journal, but has not been fully edited. Content may change prior to final publication. Citation information: DOI 10.1109/TII.2018.2818153, IEEE Transactions on Industrial Informatics

Table 1: Parameter Values of Induction Motor

Descriptions	Parameters	Nominal Values
DC link Voltage	V_{dc}	582 (V)
Stator Resistance	R_s	2.68 Ω
Rotor Resistance	R_r	2.13 Ω
Inductance	L_m	275.1 (mH)
Stator Inductance	L_s	283.4 (mH)
Rotor Inductance	L_r	283.4 (mH)
Pole Pairs	P	1.0
Speed	ω_{nom}	2772.0 (RPM)
Torque	T_{nom}	7.5 (Nm)
Inertia	J	0.005 $Kg \cdot m^2$

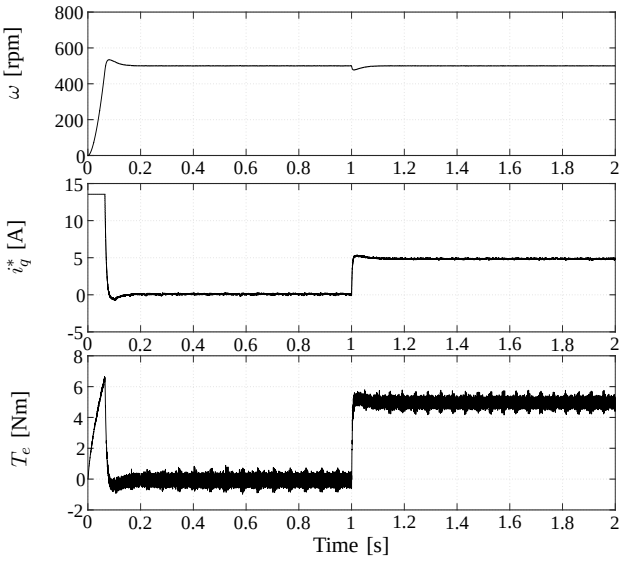

Fig. 4: Speed (ω), current (i_q^*), torque (T_e) waveforms when the rated speed is $\omega_r = 500$ rpm and the load torque is set at 5 Nm.

IV. Numerical Simulation And Experimental Results

In the following section, control performances of GPIO-PCC are illustrated using numerical simulations and experimental verification. The parameters of induction machine used in the simulation and tests are shown in Table 1. All related values are obtained from the set-up in laboratory.

A. Simulation Results

A simulation comparison is finished by a MATLAB/Simulink environment. The sample frequency is set at 16 kHz which has the same value as that in real tests. The speed reference is set to be $\omega_r = 500$ rpm.

Aiming to show the advantages of the novel GPIO-PCC method proposed in this paper. Based on the induction motor's mathematical model, torque load disturbance and a varying inertia value are considered for verifying the performance.

First, to verify the disturbance rejection of the proposed GPIO-PCC method, the load torque variation is

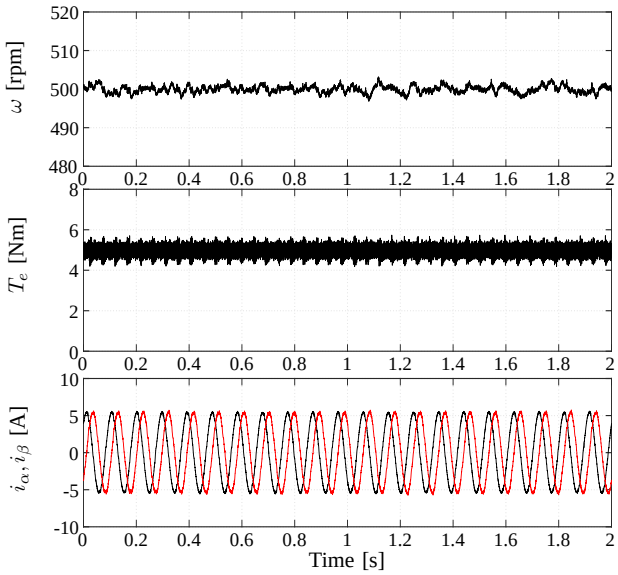

Fig. 5: Speed (ω), torque (T_e), stator current (i_α, i_β) waveforms when the rated speed is $\omega_r = 500$ rpm and the inertia value is given at $10J_{nom}$ with a 5 Nm load torque.

considered here. The parameters in GPIO-PCC controller are selected as $k_p = 0.06, \beta_1 = 10, \beta_2 = 100$. In Fig. 4, one can see that the speed response is also good when the load torque is given.

In addition, the inertia value varies here for verifying the robustness of proposed method. From Fig. 5, one can see that the closed loop performance is insured even if the inertia value is changed from J_{nom} to $10J_{nom}$ suddenly.

B. Experimental Results

The proposed GPIO-PCC method has been implemented on a test bench as shown in Fig. 6. Two 2.2 kW squirrel-cage IMs are employed. The first main motor is driven by a insulated-gate bipolar transistor gates based commercial SERVOSTAR620 14-kVA inverter, it is controlled by a 1.4 GHz real-time computer system. The control scheme can be implemented with C program on this hardware. The other load motor is controlled by a Danfoss inverter, the number is VLT FC-302 3.0-kW, it is used for loading torque suddenly. A 1024-point incremental encoder measures the rotor position. Some experimental results are compared with traditional PCC method which has been proposed in [11].

The first experimental result in Fig. 7 is to show the system operation performance of GPIO-PCC via the full speed reversal maneuver process. The response curves of speed, electromagnetic torque and stator current are presented in Fig. 7. The average switching frequency is about 3.0 kHz. During the speed dynamic response process especially when the speed is changed

This article has been accepted for publication in a future issue of this journal, but has not been fully edited. Content may change prior to final publication. Citation information: DOI 10.1109/TII.2018.2818153, IEEE Transactions on Industrial Informatics

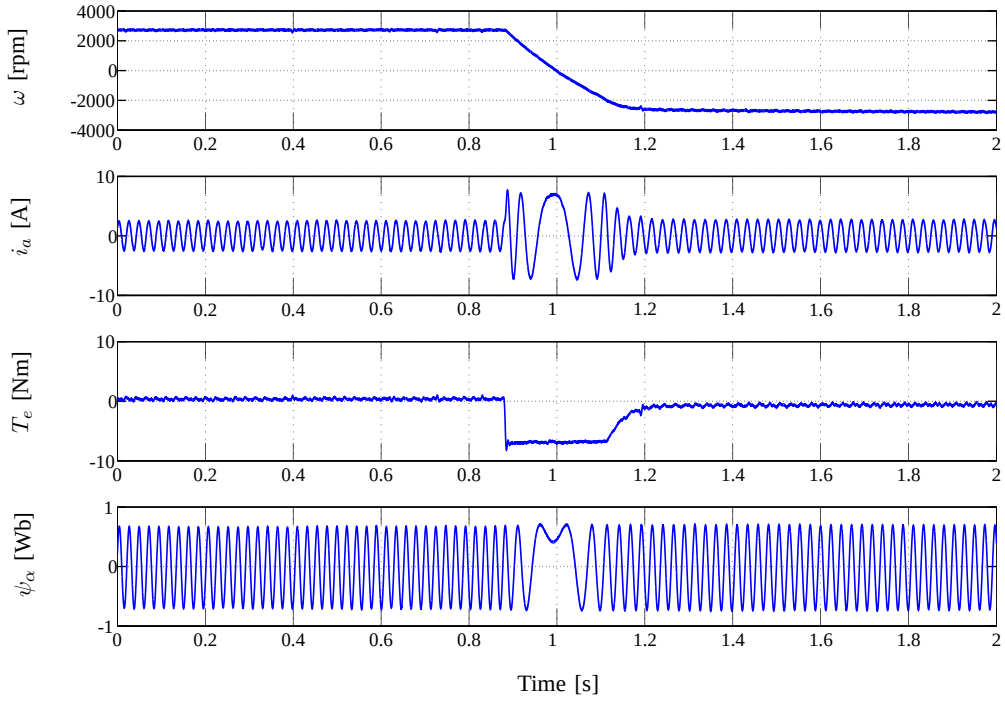

Fig. 7: Speed (ω), stator current (i_a), torque (T_e), and stator flux (ψ_α) waveforms during the full speed reversal process from 2772 rpm to -2772 rpm.

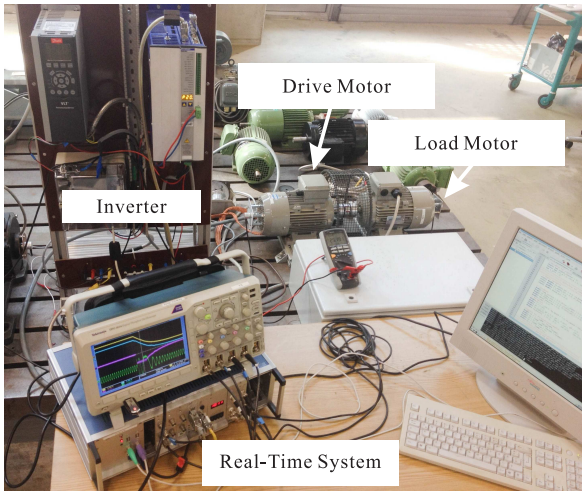

Fig. 6: Test bench description.

from 2772 rpm to -2772 rpm, the electromagnetic torque reaches its control saturation value for the shortest settling time. The response curves of stator flux in α frame and its magnitude are also given. The stator flux magnitude reference value is set as 0.71 Wb. The figure shows that the flux ripple is less than 0.02 Wb during all the speed range.

Figs. 8 and 9 show that the speed response, torque and current performances are all better. Especially from Fig. 9, we can find that the system's speed performance is also verified when the load torque is given at half load (3.75 Nm). The torque ripple is about 0.6 Nm which is better than the existed PCC method.

To verify the load torque reject ability, a full load test has been finished to demonstrate the system performance. As fig. 10, the experimental result under a sudden torque variation from 0 Nm to 7.5 Nm, that is given at the full speed reference of 2772 rpm. The torque reference which is generated by the proposed GPIO-PCC controller, changes from zero to the rated value with full load (7.5 Nm), the torque ripple is about 0.8 Nm, the steady state torque accuracy is improved. Thus, the GPIO observer-based PCC method is completely coordinated. The rise time is about 370 μs, this fast torque response is one of the advantages of this GPIO observer-based PCC control system. The speed recovery process only needs 0.42s, which is also faster than that of the traditional PCC method.

Figs. 11-14 show that when resistances of R_s, R_r, inductance L_m and the inertia value J are time varying in the low speed operation(the speed reference is 200 rpm), the closed-loop system is also stable until the inertia value is linearly increased to 1000% of the original value($J = 10J_{nom} = 0.05kg \cdot m^2$) and R_s, L_m is linearly increased to the original value of $334\%, 167\%$. For the traditional PCC method in [11], this upper limit of R_s to maintain robustness are only $160\%, 110\%$ of original value. The speed is also stable even when rotor resistance value is changed to 10Ω which is 460% of the original value. It has a strong robustness to R_r. Especially from Fig. 15, the two parameters are

This article has been accepted for publication in a future issue of this journal, but has not been fully edited. Content may change prior to final publication. Citation information: DOI 10.1109/TII.2018.2818153, IEEE Transactions on Industrial Informatics

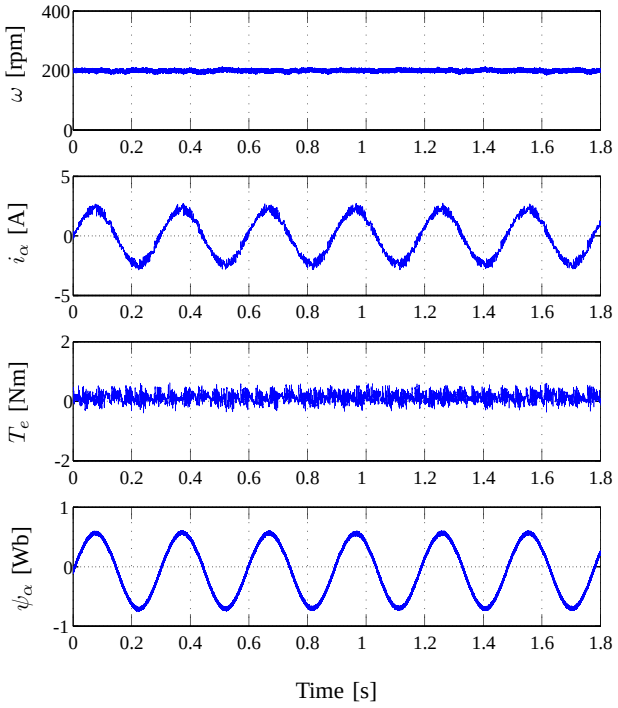

Fig. 8: Steady state: speed (ω), stator current (i_α), torque (T_e), and stator flux (ψ_α) responses when the speed reference is 200rpm (load torque is set as 0 Nm).

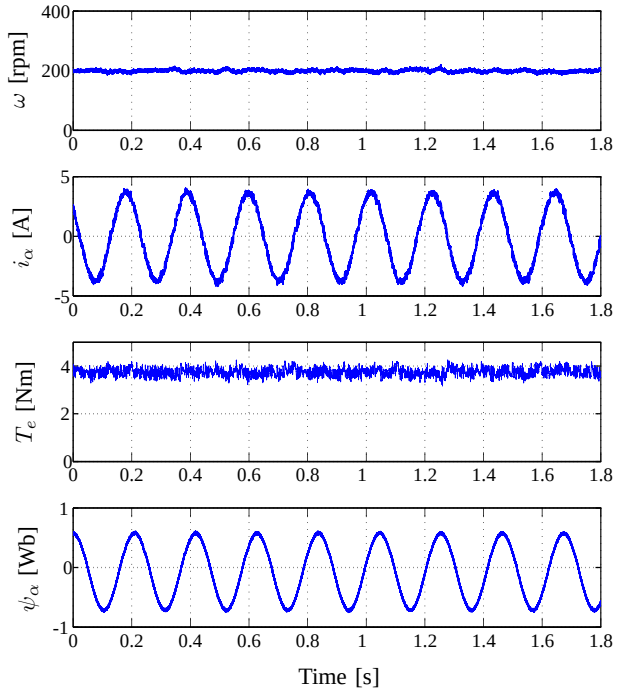

Fig. 9: Steady state: speed (ω), stator current (i_α), torque (T_e), and stator flux (ψ_α) responses when the speed reference is 200rpm (load torque is given at 3.75 Nm).

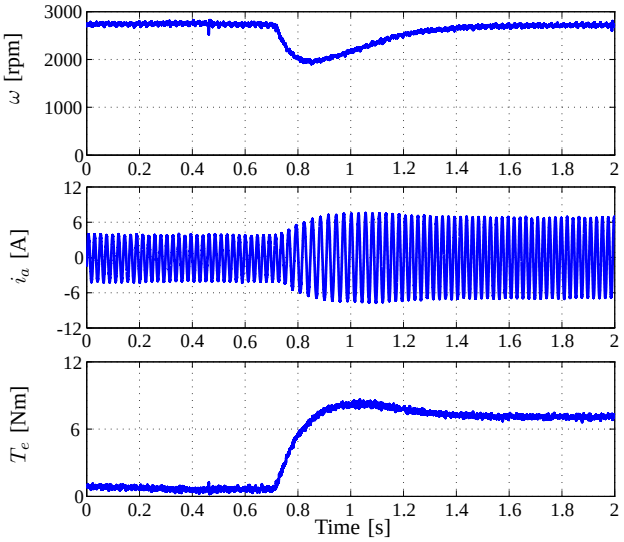

Fig. 10: Dynamic response: speed (ω), stator current (i_a) and torque (T_e) responses when the speed reference is 2772 rpm and the load torque is 7.5 Nm.

Table 2: Performance comparison of PCC and GPIO-PCC

Descriptions	**PCC**	**GPIO-PCC**
Speed ω_{nom} Recovery Time	Large	Small
Torque Ripple T	Large	Small
Inductance L_m	Low	High
Rotor Resistance R_s	Low	High
Stator Resistance R_r	Low	High
Inertia J	Low	High

varying at the same time for testing the performance. In this test, we assume that the Rr changes with the same react as R_s. It could be seen that within about twice of original values, the system is under control. At around 1.5s time instant, the system losses the stability. Generally, the system has a wide robustness range for the variation of R_s and R_r together. From the above comparison of experimental results, compared with the traditional PCC method described as [11], the induction motor system robustness is improved by the proposed control method.

As details in Table 2, we have the same conclusion that not only the load torque disturbance rejection ability is markedly improved, but also the system robustness is enhanced by the proposed GPIO-PCC method. The system dynamic response and steady state performance are also insured. It should notice that the GPIO-PCC control scheme could improve robustness and disturbance rejection ability without sacrificing the system nominal performance.

V. Conclusion

A GPIO observer based robust PCC solution for induction motor systems has been studied for improving the system's disturbance rejection and robustness

This article has been accepted for publication in a future issue of this journal, but has not been fully edited. Content may change prior to final publication. Citation information: DOI 10.1109/TII.2018.2818153, IEEE Transactions on Industrial Informatics

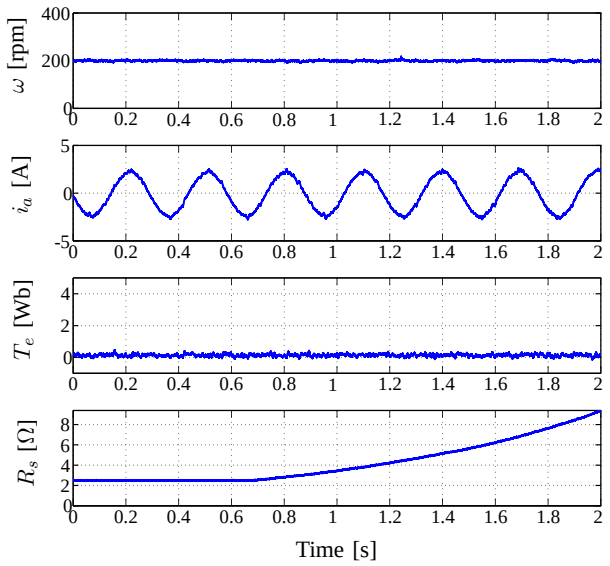

Fig. 11: Robustness: speed (ω) (the speed reference is 200 rpm), stator current (i_a), torque (T_e), and stator resistance(R_s) responses.

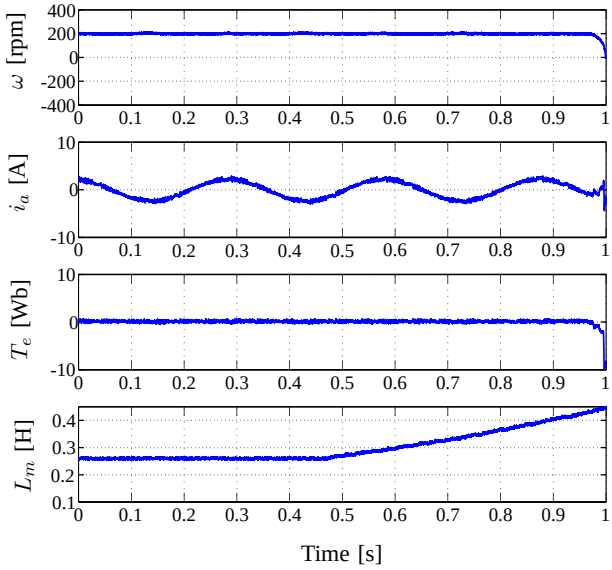

Fig. 13: Robustness: speed (ω) (the speed reference is 200 rpm), stator current (i_a), torque (T_e), and inductance value (L_m) responses.

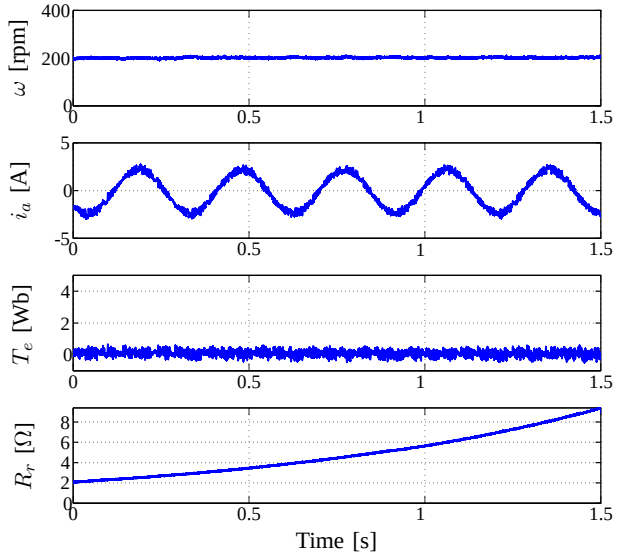

Fig. 12: Robustness: speed (ω) (the speed reference is 200 rpm), stator current (i_a), torque (T_e), and rotor resistance (R_r) responses.

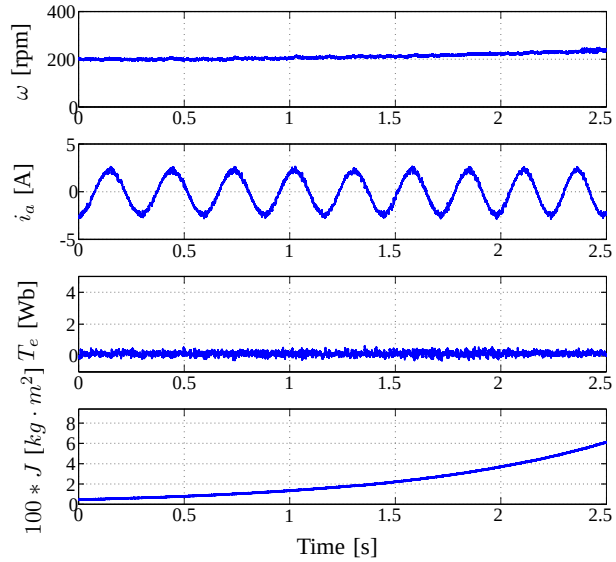

Fig. 14: Robustness: speed (ω) (the speed reference is 200 rpm), stator current (i_a), torque (T_e), and inertia value ($100 * J$) responses.

in this paper. Not only does the speed loop utilize the time-varying disturbance estimation based feed-forward compensation solution, but also the flux and current prediction use this technique. The system stability analysis with proposed GPIO-PCC method has also been given. The simulation and experimental results have shown that not only a better tracking performance is confirmed, but also the closed loop system obtains a better disturbance rejection against torque load variation and time-varying parameter uncertainties.

REFERENCES

[1] D. Casadei, F. Profumo, G. Serra, et al. “FOC and DTC: two viable schemes for induction motors torque control,” *IEEE Trans. Power Electron.*, vol. 17, no. 5, pp. 779-787, Sep. 2002.

[2] G. Pellegrino, E. Armando, P. Guglielmi. “Direct flux field-oriented control of IPM drives with variable DC link in the field-weakening region,” *IEEE Trans. Ind. Appl.*, vol. 45, no. 5, pp. 1619-1627, Aug. 2009.

[3] Y. Zhang, J. Zhu, Z. Zhao, et al. “An improved direct torque control for three-level inverter-fed induction motor sensorless drive,” *IEEE Trans. Power Electron.*, vol. 27, no. 3, pp. 1502-1513, Mar. 2012.

This article has been accepted for publication in a future issue of this journal, but has not been fully edited. Content may change prior to final publication. Citation information: DOI 10.1109/TII.2018.2818153, IEEE Transactions on Industrial Informatics

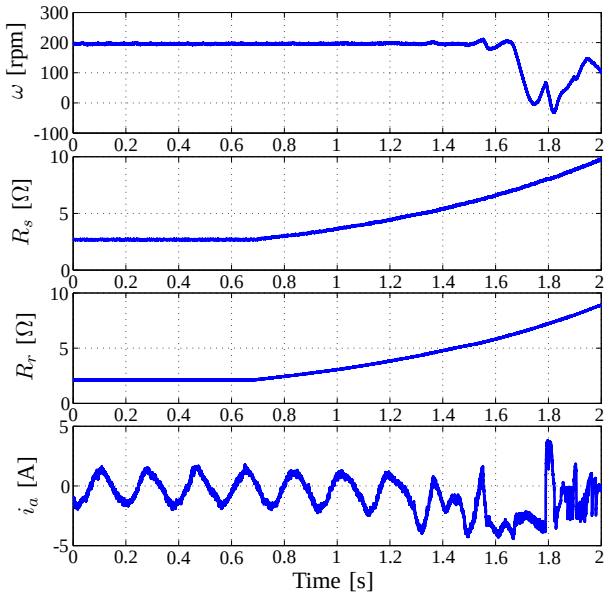

Fig. 15: Robustness: speed (ω) (the speed reference is 200 rpm), stator resistance (R_s), rotor resistance (R_r), stator current (i_a) responses.

[4] P. Cortes, P. Kazmierkowski, R. Kennel, D. Quevedo, and J. Rodriguez, "Predictive control in power electronics and drives," *IEEE Trans. Ind. Electron.*, vol. 55, no. 12, pp. 4312-4324, Dec. 2008.

[5] M. Nemec, D. Nedeljkovic, and V. Ambrozic, "Predictive torque control of induction machines using immediate flux control," *IEEE Trans. Ind. Electron.*, vol. 54, no. 4, pp. 2009-2017, Aug. 2007.

[6] M. Preindl, S. Bolognani, "Model predictive direct speed control with finite control set of PMSM drive systems," *IEEE Trans. Power Electron.*, vol. 28, no. 2, pp. 1007-1015, Feb. 2013.

[7] T. Geyer "Computationally efficient model predictive direct torque control," *IEEE Trans. Power Electron.*, vol. 26, no. 10, pp. 2804-2816, Oct. 2011.

[8] R. Vargas, U. Ammann, B. Hudoffsky, and J. Rodriguez, "Predictive torque control of an induction machine fed by a matrix converter with reactive input power control," *IEEE Trans. Power Electron.*, vol. 25, no. 6, pp. 1426-1438, June 2010.

[9] T. Geyer, G. Papafotiou, M. Morari. "Model predictive direct torque control-part I: concept, algorithm, and analysis," *IEEE Trans. Ind. Electron.*, vol. 56, no. 6, pp. 1894-1905, June 2009.

[10] T. Geyer. "Model predictive direct torque control: derivation and analysis of the state-feedback control law," *IEEE Trans. Ind. Appl.*, vol. 49, no.5, pp. 2146-2157, Sept. 2013.

[11] F. Wang, S. Li, X. Mei, et al. "Model based predictive direct control strategies for electrical drives: an experimental evaluation of PTC and PCC Methods," *IEEE Trans. Ind. Informat.*, vol. 11, no.3, pp. 671-681, June 2015.

[12] J. Holtz "Advanced PWM and predictive control-an overview," *IEEE Trans. Ind. Appl.*, vol. 63, no. 6, pp. 3837-3844, May 2016.

[13] J. Rodriguez, J. Pontt, C. Silva, P. Correa, P. Lezana, P. Cortes, and U. Ammann. "Predictive current control of a voltage source inverter," *IEEE Trans. Ind. Electron.*, vol. 54, no.1, pp. 495-503, Feb. 2007.

[14] H. Young, M. Perez, J. Rodriguez. "Analysis of finite-control-set model predictive current control with model parameter mismatch in a three-phase inverter," *IEEE Trans. Ind. Electron.*, vol. 63, no. 5, pp. 3100-3107, May 2016.

[15] T. Geyer , D. E. Quevedo. "Performance of multistep finite control set model predictive control for power electronics," *IEEE Trans. Power. Electron.*, vol. 30, no. 3, pp. 1633-1644, March 2015.

[16] T Geyer, D. E. Quevedo. Multistep finite control set model predictive control for power electronics. *IEEE Trans. Power Electron.*, vol.29, no.12, pp.6836-6846, Dec. 2014.

[17] K. S. Low, H. Zhuang, "Robust model predictive control and observer for direct drive applications," *IEEE Trans. Power Electron.*, vol. 15, no. 6, pp. 1018-1028, Nov. 2000.

[18] M. J. Youn. "A nonlinear speed control for a PM synchronous motor using a simple disturbance estimation technique," *IEEE Trans. Ind. Electron.*, vol. 49, no. 3, pp. 524-535, June 2002.

[19] J. Han, "From PID to active disturbance rejection control," *IEEE Trans. Ind. Electron.*, vol. 56, no. 3, pp. 900-906, March 2009.

[20] S. Li, Z. Liu. "Adaptive speed control for permanent-magnet synchronous motor system with variations of load inertia," *IEEE Trans. Ind. Electron.*, vol. 56, no. 8, pp. 3050-3059, Aug. 2009.

[21] H. Liu, S. Li. "Speed control for PMSM servo system using predictive functional control and extended state observer," *IEEE Trans. Ind. Electron.*, vol. 59, no. 2, pp. 1171-1183, Feb. 2012.

[22] W. Chen, "Disturbance observer based control for nonlinear systems," *IEEE/ASME Trans. Mechatron.*, vol. 9, no. 4, pp. 706-710, Dec. 2004.

[23] S. Li, J. Yang, W. Chen, X. Chen. *Disturbance observer-based control: methods and applications*, CRC press, 2014.

[24] H. Siara-Ramírez, M. A. Oliver-Salazar. "On the robust control of buck-converter dc-motor combinations," *IEEE Trans. Power Electron.*, vol. 28, no. 8, pp. 3912-3922, Aug. 2013.

[25] B. Sun and Z. Gao, "A DSP-based active disturbance rejection control design for a 1-kW H-bridge DC-DC power converter," *IEEE Trans. Ind. Electron.*, vol. 52, no. 5, pp. 1271-1277, Oct. 2005.

[26] M. Nakao, K. Ohnishi, K. Miyachi. "Robust decentralized joint control based on interference estimation," *in Robotics and Automation, 1987 IEEE International Conference on*, vol. 4, pp. 326-331.

[27] J. Wang, F. Wang, Z. Zhang, et al. "Design and implementation of disturbance compensation-based enhanced robust finite control set predictive torque control for induction motor systems." *IEEE Trans. Ind. Informat.*, 13(5): 2645-2656, 2017.

[28] H. Khail. *Nonlinear Systems*, 3rd ed. Upper Saddle River, NJ, USA: Prentice-Hall, 2002.

This article has been accepted for publication in a future issue of this journal, but has not been fully edited. Content may change prior to final publication. Citation information: DOI 10.1109/TII.2018.2818153, IEEE Transactions on Industrial Informatics

Junxiao Wang (S'14-M'18) was born in Wuxue, Hubei Province, China in 1986. He received his B.S. and M.S. degrees in Information Engineering College of Henan University of Science and Technology (HAUST), Luoyang, China in 2008 and 2011, respectively. He was a visiting Ph.D. student in the Institute for Electrical Drive Systems and Power Electronics at Technical University of Munich (TUM) in Germany from Sep. 2015 to Sep. 2016. In 2017, he received his Ph.D. degree in control theory and control engineering from School of Automation, Southeast University (SEU), Nanjing, China. Currently he is working in College of Information Engineering, Zhejiang University of Technology. His research interests include advanced control theory and its application to power electronics and AC motor control systems.

He was the recipient of the IET Premium Awards from the IET Control Theory & Application in 2017.

Fengxiang Wang (S'13-M'14) was born in Jiujiang,China, in 1982. He received the B.S. degree in electronic engineering and the M.S. degree in automation from Nanchang Hangkong University, Nanchang, China, in 2005 and 2008, respectively. In 2014, he received Ph.D. degree at the Institute for Electrical Drive Systems and Power Electronics, Technische Universitaet Muenchen, Munich, Germany. Currently he is working at Haixi Institutes, Chinese Academy of Sciences, China. His research interests include predictive control and sensorless control for electrical drives.

Gaolin Wang (M13) received the B.S., M.S. and Ph.D. degrees in Electrical Engineering from Harbin Institute of Technology, Harbin, China, in 2002, 2004 and 2008 respectively. In 2009, he joined the Department of Electrical Engineering, Harbin Institute of Technology as a Lecturer, where he has been a Full Professor of Electrical Engineering since 2014. From 2009 to 2012, he was a Postdoctoral Fellow in Shanghai Step Electric Corporation, where he was involved in the traction machine control for direct-drive elevators. He has authored more than 60 technical papers published in journals and conference proceedings. He is the holder of 10 Chinese patents. His current major research interests include permanent magnet synchronous motor drives, high performance direct-drive for traction system, position sensorless control of AC motors, efficiency optimization control of PMSM, and digital control of power converters. Dr. Wang serves as an Associate Editor of IET Electric Power Applications, and Journal of Power Electronics. He received the Outstanding Research Award and the Delta Young Scholar Award from the Delta Environmental and Educational Foundation in 2012 and 2014, respectively. He is currently supported by the National Natural Science of China for Excellent Young Scholars, the Program for Basic Research Excellent Talents and the Young Talent Program from Harbin Institute of Technology.

Shihua Li (M'05-SM'10) was born in Pingxiang, Jiangxi Province, China in 1975. He received his bachelor, master, Ph.D. degrees all in Automatic Control from Southeast university, Nanjing, China in 1995, 1998 and 2001, respectively. Since 2001, he has been with School of Automation, Southeast University, where he is currently a professor and the director of Mechatronic Systems Control Laboratory. He has authored or coauthored over 200 technical papers and two books. His main research interests lie in modeling, analysis and nonlinear control theory with applications to mechatronic systems.

Prof. Li is the Vice chairman of IEEE CSS Nanjing Chapter. He serves as associate editors or editors of International Journal of Robust & Nonlinear Control, IET Power Electronics, International Journal of Control, Automation and Systems, International Journal of Electronics, and guest editors of IEEE Transactions on Industrial Electronics, International Journal of Robust & Nonlinear Control and IET Control Theory & Applications.

Li Yu (M09) received the B.S. degree in control theory from Nankai University, Tianjin, China, in 1982, and the M.S. and Ph.D. degrees from Zhejiang University, Hangzhou, China. He is currently a Professor in College of Information Engineering, Zhejiang University of Technology. He has authored or co-authored three books and over 200 journal or conference papers. His current research interests include wireless sensor networks, networked control systems and motion control.